

Research Article

Viscoelastic Analysis of the Damping Asphalt Mixtures (DAMs) Made with a High Content of Asphalt Rubber (AR)

Jiandong Huang  and Yuantian Sun 

School of Mines, China University of Mining and Technology, Xuzhou 221116, China

Correspondence should be addressed to Yuantian Sun; yuantiansun@cumt.edu.cn

Received 15 September 2020; Revised 4 October 2020; Accepted 15 October 2020; Published 28 October 2020

Academic Editor: Shaopeng Wu

Copyright © 2020 Jiandong Huang and Yuantian Sun. This is an open access article distributed under the Creative Commons Attribution License, which permits unrestricted use, distribution, and reproduction in any medium, provided the original work is properly cited.

Damping asphalt mixtures (DAMs) have been developed to resist vibration and noise caused by traffic loads, and the ultimate design goal in this process is to increase damping. However, while optimizing its damping characteristics, the viscoelastic properties are not yet clear. In the present study, two DAMs are designed based on the open-graded (OG) aggregate structure, and the viscoelastic properties are evaluated subsequently by the dynamic mechanical testing. The results show that the proposed mix-design method for DAMs can meet the mechanical requirements specified in the standards; DAMs are detected to have higher phase angle and lower stiffness modulus compared with traditional mixtures, and the antifatigue performance is excellent but resistance to rutting may face challenges.

1. Introduction

Today, complex transportation networks have become a symbol of urbanization. The convenient transportation has enriched people's lives. However, traffic-induced vibration from traffic networks is around everyone in the city, which can affect the living conditions of urban residents and can lead to sleep disorders, and is becoming more and more serious [1–4]. Vibrations are to be reduced also in the case of sensitive scenarios as hospitals, scientific research labs, and high-tech industries [5–7]. Furthermore, road vibrations induced by traffic generate noise dominating to frequencies below 1000 Hz [8].

The problem is particularly relevant when pavement surfaces are uneven like in the case of stone pavements or artificial bumps [5, 9]. Discrete, periodic, and random irregularities on the road surface and defects in the vehicle itself lead to dynamic interaction forces between the vehicle and the road. Vibration caused by road traffic is an environmental issue of worldwide concern. The vibratory mechanism affects the quality of life of people daily and nightly hours. Such annoyance shall not be underestimated since it could be the cause of stress-related human diseases

[2, 3]. Traffic-induced vibration can jeopardize the integrity and the stability of historical buildings. Vibrations are to be reduced also in the case of sensitive scenarios as hospitals, scientific research labs, and high-tech industries [5–7].

To mitigate the effects of traffic-induced vibration, various preventive strategies are under investigation. Limiting traffic volumes and speed, screening of vibration by using in-ground barriers, and developing isolation systems represent some of the methods proposed [5]. In the field of pavement engineering, the damping properties of viscoelastic materials included in asphalt mixtures are under investigation to reduce vibrations. According to the study by Hanazato et al. [10], the increase in damping of pavement materials can reduce ground vibrations into the loading area and within the corresponding surrounding region. This improvement is critical for reducing vibrations to improve the quality of life and to preserve the stability of buildings [11].

The effect of the composition of asphalt mixtures on the damping properties has been evaluated in several studies in the fields of pavements and railway track-bed engineering [12–21]. Results have highlighted that the use of crumb rubber (CR) from the end of life tires (ELTs) in asphalt mixtures provides a higher damping response than

conventional ones. Biligiri [22] used the phase angle as an indicative of noise-damping characteristics in the field. This author continued his investigation about the effect of pavement materials' damping properties concluding that rubberized mixtures with the extra binder, higher porosity, and rubber inclusions provide sufficient extra viscodamping effect, higher noise-absorption potential, and higher vibroacoustic damping capacity. Studies conducted by Li et al. [23] with the approach of free attenuation vibration tests concluded that damping ratio of asphalt mortar beam specimen increased with the increase of crumb rubber amount, and the addition of the crumb rubber particles can improve the damping performance for better usage in energy absorption and vibration attenuation. Wang and Hoeg [14] also reported that an increase in rubber content from 30% to 80% increased damping by about 20% in waste granular rubber and cement-stabilized mixtures. In the case of railway track-bed engineering, the use of damping materials by rubberized mixture has been investigated as a replacement of basalt in the foundation [24]. In this study, a resonance column test was conducted to measure the stiffness and damping ratio of rubber-modified asphalt mixtures prepared with different rubber contents. Findings highlighted that rubberized-mixtures can be used in the foundation of railway track-bed for high-speed trains to reduce vibration due to their damping properties. In 2018, Huang and co-workers [25, 26] presented a theoretical model to predict the damping ratio of a road pavement specifically designed to mitigating traffic-induced vibrations. The pavement was composed of the so-called damping asphalt mixtures (DAMs) at the interface between the binder and the base layer. Based on model results, to achieve a decrease of vibration accelerations at the soil surface away from the wheel track, the much higher damping property of the asphalt mixture compared to that of a conventional one is required.

One way to increase the damping properties of the DAMs is to use higher volumes of asphalt rubber (AR) compared to hot mix asphalt (HMA) prepared with traditional crumb rubber modifier (CRM) binder [27]. For this reason, the design of the DAM has the scope to accommodate a sufficient volume of AR to increase damping, while maintaining adequate stability and resistance. Using OG aggregate structure can allow a large volume of voids in mineral aggregates (VMAs) and provide the aggregate interlock by angular tough basalt aggregates, meeting the design scope of DAMs [26]. Traditionally, such aggregate structure is designed to achieve a volume of air voids in compacted mixtures between 20 and 25% to provide adequate drainage and noise absorption. The large VMA available needs to be filled with AR to increase the volume of effective bitumen (V_{be} , bitumen not absorbed in mineral aggregates), which is representative of the thickness of the film of mortar (bitumen + filler) that coats the mineral coarse and fine aggregates [28].

Higher values of VMA and V_{be} are likely to increase the durability of mixtures providing a higher fatigue resistance and a lower oxidative susceptibility [29]. However, the excessive binder content may affect the stability of the mixtures

at high temperatures worsening their rutting resistance [30]. Therefore, the analysis of fatigue and rutting performance of DAMs is currently unknown. The viscoelasticity of rubberized and nonrubberized asphalt mixtures has been analyzed in the previous literature. However, due to the higher AR contained in DAMs, the difference between its viscoelasticity and conventional asphalt mixtures is not clear yet.

2. Research Objectives

The research objective of the present study is to focus on the evaluation of the viscoelastic properties of the DAMs used for the damping layers in road pavements, with the approach of the dynamic mechanism testing. Dynamic modulus, phase angle and their master curves, fatigue parameter, and rutting parameter will be analyzed as factors for viscoelasticity analysis. At the same time, in order to verify the feasibility of the proposed mix-design method for DAMs, the basic mechanical properties will also be characterized and compared with the requirements of the specification.

3. Experimental Tests

3.1. Materials. AR produced according to the so-called wet process (WP) by mixing a Pen 50–70 base asphalt with 20% of CRM was used as the binder. The gradation of the CRM particles is given in Figure 1.

The dry mix was constituted of basalt coarse aggregates, natural sand, and mineral filler. The physical properties of the aggregates are given in Table 1.

3.2. Mixture Design. An open-graded (OG) mixture named as the reference mixture (Mix ref) was selected as the starting for the design of the dedicated mixes for the damping layer. The nominal maximum size (NMS) of the aggregate was 8 mm, in line with the optimized design thickness of the damping layer of 3 cm [26]. The OG mix has been optimized and evaluated in a previous study, showing the desired mechanical properties. Starting from the Mix ref, two DAMs (named as Mix 1 and Mix 2, respectively) were designed in the present study. They contain a higher asphalt content compared to the Mix ref (+9.8% and +15.0% by weight of aggregates for Mix 1 and Mix 2, respectively). The amount of binder in the mix has been increased as long with the amount of filler. The aggregate gradations of the Mix ref and the DAMs (Mix 1 and Mix 2) are shown in Figure 2.

Table 2 presents the volumetric parameters and the corresponding parameters in weight (if available) for Mix ref, Mix 1, and Mix 2. Mix 1 and Mix 2 have a higher amount of filler compared to the reference mixture (Table 2) (+9.8% and +15.0% in weight, respectively). It has to be noted that the filler and binder have been increased by maintaining the same D/P proportion (~ 1) of Mix ref. This aspect is relevant since it indicates that the amount of binder has been maximized by maintaining the same volume fraction of filler in the mastic. The cross section of the mixes is presented in Figure 3.

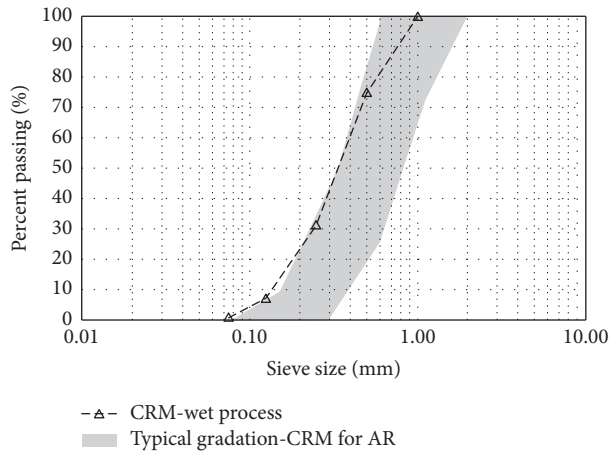


FIGURE 1: Gradation of rubber particles.

TABLE 1: Physical properties of aggregates (EN 1097-6/7).

Properties	Basalt	Sand	Mineral filler
Bulk specific gravity (G_{sb}) (kg/m^3)	2.753	2.629	2.710
Water absorption (%)	1.39	0.86	—
Soundness, magnesium sulphate solution (%)	≤ 15	0.2	ASTM C 88

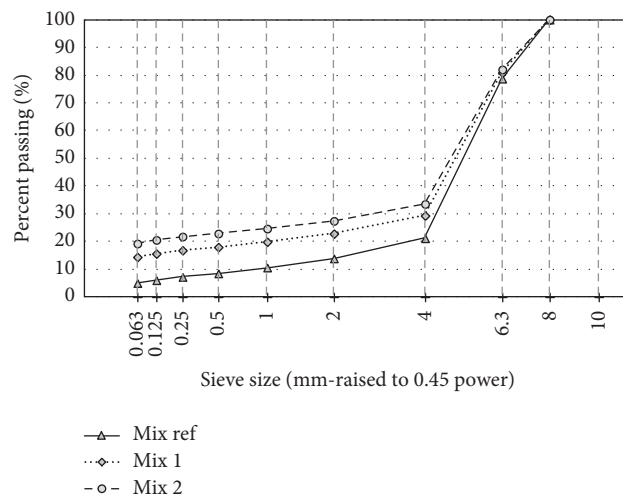


FIGURE 2: Aggregate gradations of mix ref, Mix 1, and Mix 2.

TABLE 2: Volumetric properties at maximum gyration numbers (by weight (W) and by volume (V) for mix 1 and mix 2 (EN 12697—parts 5, 6, and 7)).

Mix		Aggregates (%)	Filler (%)	Binder (%)	VA (%)	VMA (%)	VFA (%)	D/P (-)
Mix ref	W	95.2	4.8	5.0	26.8	35.2	23.8	0.96
	V	61.7	3.1	8.4				
Mix 1	W	85.3	14.7	14.8	0.4	28.0	98.4	0.99
	V	61.4	10.6	27.6				
Mix 2	W	80.2	19.8	20.0	0.1	34.2	99.6	0.99
	V	52.8	13.0	34.1				

VA: air voids; VMA: voids in mineral aggregates; VFA: voids filled with asphalt; D/P: dust to binder ratio.

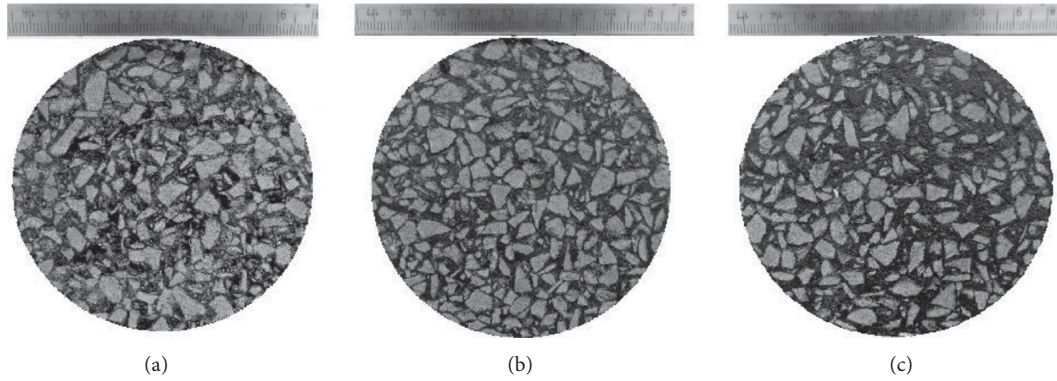


FIGURE 3: Cross section of the mixes. (a) Mix ref, (b) Mix 1, and (c) Mix 2.

3.3. Experimental Program and Methods. The experimental program is divided into two phases: evaluating the mix-design properties and characterizing the dynamic mechanical properties.

3.3.1. Mix-Design Properties. The mix-design properties are evaluated by the means of indirect tensile strength (ITS) test. The details of the experimental program are given below. The ITS test was conducted on 100 mm diameter compacted samples (using SGC according to EN 12697–31). For the SGC process, it should be noted that the traditional gyration number of 50 was employed for the Mix ref and Mix 1. However, for Mix 2, the gyration number of 2 that can already meet the compaction requirements is selected to prevent the excessive compaction caused the asphalt to seep out of the mold. Mixing and compaction temperatures were kept at 180°C, and the samples were tested at two conditions by using three replicates for each condition. The first is the dry condition, which is conducted on dry samples conditioned at 25°C according to EN 12697–23. The second is the wet condition that is conducted at 25°C on samples conditioned in a water bath at 40°C for 72 hours according to EN 12697–12.

The ITS is measured both in dry (ITS_d) and wet (ITS_w) conditions, and the ratio between the values at the two conditions is a measure of the moisture resistance of the mixture intended as the loss in tensile strength due to the effects of water (indirect tensile strength ratio, ITSR).

3.3.2. Dynamic Mechanical Testing. The dynamic mechanical properties of the different mixtures were measured according to the AASHTO TP 79-12 standard, using the asphalt mixture performance tester (AMPT). In the procedure to evaluate the dynamic mechanical properties, the specimen at specific testing temperatures is subjected to a controlled sinusoidal (haversine) compressive stress of varying frequencies. The applied stresses and measured axial strains are determined as a function of time and used to calculate the dynamic modulus and phase angle.

In the present study, two specimens at the target air void are prepared in accordance with the AASHTO PP60 standard. For each mixture, the superpave gyration compactor

(SGC) specimen with diameter of 150 mm and height of 180 mm was prepared firstly according to the requirements of AASHTO T312 standard, as presented in Figure 4. The testing specimen is then sawed and cored from the SGC specimen to a diameter of 100 mm and height of 150 mm, in order to ensure the smooth surface and uniform ends with minimal or no surface irregularities after the sawing process. It should be noted the mass of each mixture should be determined according to the SGC specimen height, G_{mm} , and target air void (which were determined in § 3.2).

The test specimen instrumentation is conducted by the so-called standard glued-gauge-point system, as presented in Figure 5. The gauge length should be confirmed as $70 \text{ mm} \pm 1 \text{ mm}$, which is measured from the center positions of the two gauge points. A total of six gauge points were attached to a specimen in the present study. Three strain gauges on the same horizontal surface were attached at intervals of 120° considering the cross section of the sample.

The dynamic modulus system is presented in Figure 6, and the testing method to describe the procedures for measuring the dynamic modulus and phase angle are given below.

A Teflon sheet with thickness of 0.25 mm was selected as the end-friction reducer and cut to a size slightly larger than the loading platen. The sample should be assembled with the platens according to the order: bottom loading platen, bottom Teflon sheet, sample, top Teflon sheet, and top loading platen. It should be noted that the top loading platen should be ensured to rotate freely during the loading process.

The testing conditions including the temperatures, loading frequencies, strain level, and confinement are reported in Table 3.

The master curves of the dynamic modulus ($|E^*|$) and the phase angle (δ) were developed under the applicability of the time-temperature superposition principle (TTSP) [31]. Horizontal shift factors were calculated by the WilliamLandelFerry (WLF) equation:

$$\log \alpha_T = -\frac{C_1 \cdot (T - T_{ref})}{C_2 + (T - T_{ref})}, \quad (1)$$

where α_T is the shift factor; C_1 and C_2 are model parameters which are determined to fit the data; T_{ref} is the reference

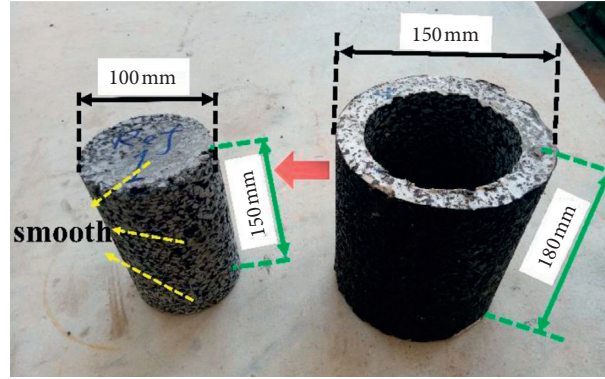


FIGURE 4: Sample preparation.

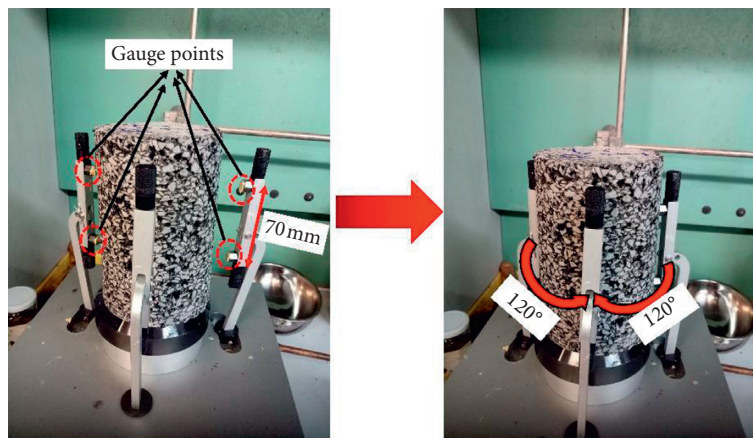


FIGURE 5: Standard glued-gauge-point (GGP) system.

temperature (selected as 20°C in the present study); and T is the testing temperature. The dynamic modulus ($|E^*|$) and the phase angle (δ) data were modeled by using the modified Christensen-Anderson-Marasteanu (CAM) model [32].

The $|E^*|$ master curve of the CAM model is given by equation (2):

$$|E^*| = E_e + \frac{E_g - E_e}{[1 + (f_c/f_r)]^{(m_e/k)}}, \quad (2)$$

where $|E^*|$ is the dynamic modulus and E_e is the equilibrium modulus that represents the stiffness modulus when the loading frequency tends to 0. In the case of DAMs, its value is considered to depend on the ultimate aggregate interlock when the contribution of the binder (or the mastic) results negligible; E_g is the glassy modulus, which represents the stiffness modulus when the loading frequency tends to infinity. Its value represents the horizontal asymptote in the high-frequency region; f_r is the reduced frequency; f_c is a location parameter that has the dimension of frequency. It is known as crossover frequency, which is the one when the storage modulus (E') is equal to the loss modulus (E''); m_e and k are the shape dimensionless parameters.

The phase angle master curve can also be obtained through the CAM model by equation (3):

$$\delta = 90I - (90I - \delta_m) \left[1 + \left(\frac{\log(f_d/f_r)}{R_d} \right)^2 \right]^{- (m_d/2)}, \quad (3)$$

$$\begin{cases} I = 0, & \text{for mixes,} \\ I = 0, & \text{if } f_r > f_d, \\ I = 1, & \text{if } f_r < f_d, \end{cases}$$

where δ is the phase angle and δ_m is the phase angle value at f_d . In the case of mixtures, it represents the maximum phase angle value and f_d is the location parameter with dimension of frequency. It is the frequency at which δ_m occurs; f_r is the reduced frequency. The measure of the phase angle is critical because it represents a measure of the internal damping. High values of phase angle imply high internal friction and therefore more dissipative behaviour under loading (a more viscous behaviour). On the other side, lower values of phase angle denote a more elastic response of viscoelastic materials, which indicates the higher capacity of storing energy under loading cycles.

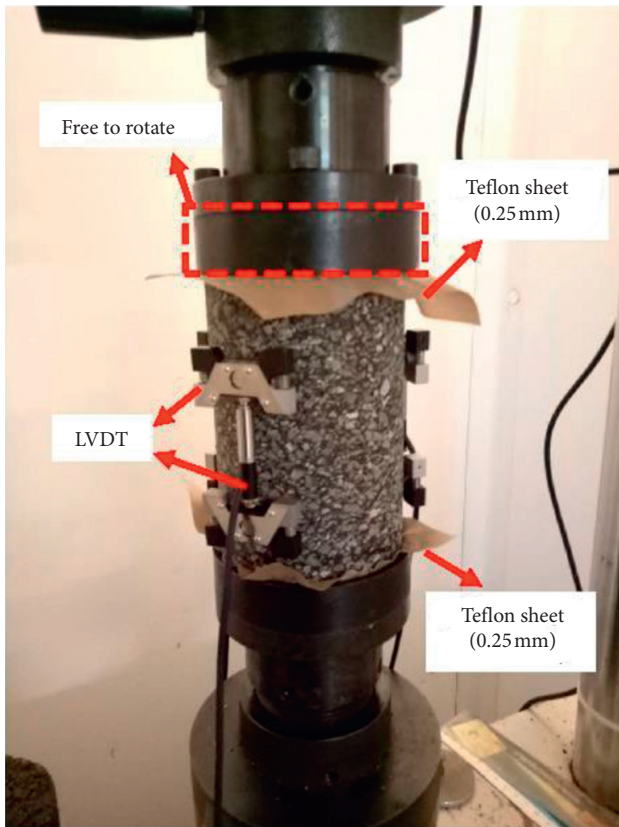


FIGURE 6: Dynamic modulus test system.

TABLE 3: Testing conditions of the dynamic mechanical test.

Test conditions	Configuration
Test temperature ($^{\circ}\text{C}$)	5, 20, 31
Loading frequency (Hz)	0.1, 0.5, 1, 2, 5, 10, 20, 25
Strain level	100 μs
Confinement	Unconfined conditions

4. Results and Discussion

4.1. Mix-Design Properties. Results of the ITS test conducted on dry- and wet-conditioned samples are given in Table 4. The replicates for each mixture and test were used. The mix-design properties, including the ITS and ITS_R values of the mixtures, are compliant with the specification at both the dry and wet conditions, clearly showing that no problems pertaining to cracking and moisture susceptibility arising for the designed DAMs. At the same time, the reliability of the mix-design method specially used for DAMs can be verified.

The reduction in the ITS_{dry} values of Mix 1 and Mix 2, compared with Mix_{ref} can be attributed to the high volume of asphalt, which can reduce the aggregate interlock affecting the tensile strength. On the other hand, a higher amount of binder (and filler) tends to increase the thickness of the mastic film coating the aggregates. This results in higher ITS_R values of Mix 1 and Mix 2 in comparison with Mix_{ref}. Besides this, a more than adequate resistance depends on the use of rubberized binder, whose reduced moisture susceptibility has been proven by several studies [33, 34].

4.2. Dynamic Modulus and Phase Angle. The master curves of the dynamic modulus ($|E^*|$) and the phase angle (δ) of the mixtures are given in Figures 7 and 8, respectively. The master curves were developed on two replicates. Results show an acceptable variability with the coefficient of variation of the average between two samples below 10% for all the cases. The shift factors were optimized on the dynamic modulus master curve and were then applied to the phase-angle master curve. The CAM model provides an adequate accuracy in modelling the raw data with the R^2 coefficient being above 97% (for modulus) and 95% (for phase angle) for all mixtures.

As far as the dynamic modulus of the three mixtures is concerned, Mix_{ref} shows the highest level of stiffness in the range of reduced frequency considered (Figure 7). This aspect was expected due to the differences in the composition between the mixtures. The higher stiffness of the OG mixture is in agreement with the tensile strength values (Table 4) and depends on the higher aggregate interlock provided a thinner film of mastic. In fact, the difference between Mix_{ref} and the two DAMs is marked in the low-frequencies region where the aggregate structure is more significant than the mastic. The difference between horizontal asymptotes in this region is of multiple orders of magnitudes. Mix 1 and Mix 2 show similar levels of stiffness in the intermediate and low range of frequencies with Mix 1 becoming stiffer at lower temperatures (higher frequencies) and Mix 2 stiffer at higher temperatures (lower frequencies).

The shape of the δ master curves is typical of mixtures. At low frequencies, the response is more controlled by the aggregate skeleton and thus, it is more elastic. In terms of elastic properties, the three mixtures did not show much difference, due to the similar skeleton structure. At the intermediate-frequency region, the response is controlled by both the aggregate skeleton and the mastic showing a visible time dependency (viscoelasticity). In such region, the peak is likely to represent the threshold between the effects of the two constituents. On the right side of the peak, the mastic phase controls more the response. On the left side, it is vice versa. Mix 2 shows the peak at higher frequencies than Mix 1 and Mix_{ref}. In this case, the higher amount of binder makes the mixture more temperature-susceptible and moves the peak towards higher frequencies (or lower temperatures). In other words, Mix 2 shows higher damping at lower temperatures. However, irrespective of frequency, Mix 1 and Mix 2 display consistently higher values of phase angle than Mix_{ref}, showing a better capacity of mitigating the vibration mechanism. At the very high frequencies, the mastic becomes stiffer and more elastic lowering the phase angle. While at the intermediate region, the response is controlled by both the constituents (aggregate and binder) showing visible viscoelastic behaviour. The values of the phase angle support were the main scope of the mix design, that is, increasing the damping response of mixtures, Mix 1 and Mix 2, shows consistently higher phase angle values than the reference mixture. Higher phase angle values indicate a more viscous response under loading with a consequent higher dissipation of energy dissipation.

TABLE 4: ITS test results.

Mixtures	ITS _{dry} (MPa)	ITSR (%)	Specification for ITS _{dry} @25°C (MPa)	Specification for ITSR (%)
Mix ref	0.62 (±0.04)	82.3		
Mix 1	0.55 (±0.03)	87.3	≥0.4	≥80
Mix 2	0.41 (±0.01)	87.8		

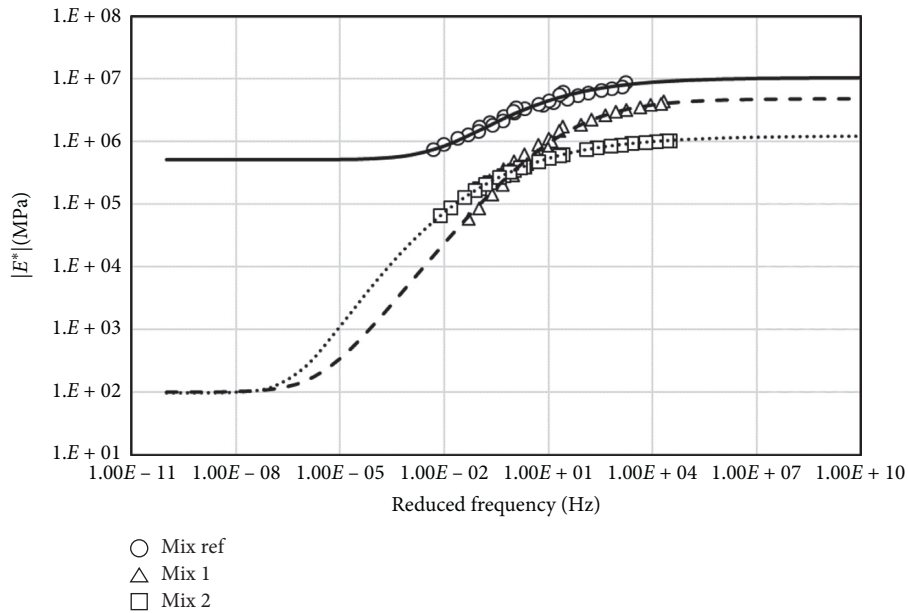


FIGURE 7: Dynamic modulus master curves.

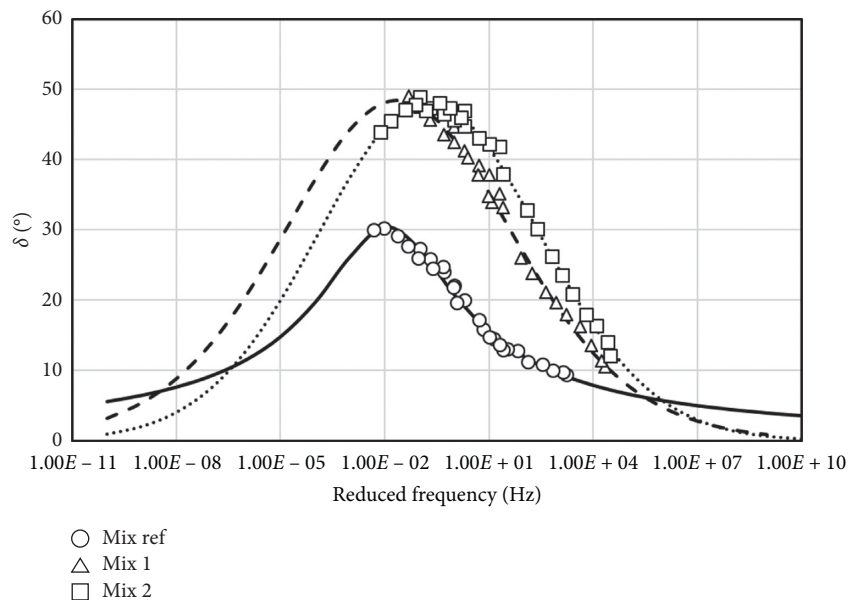
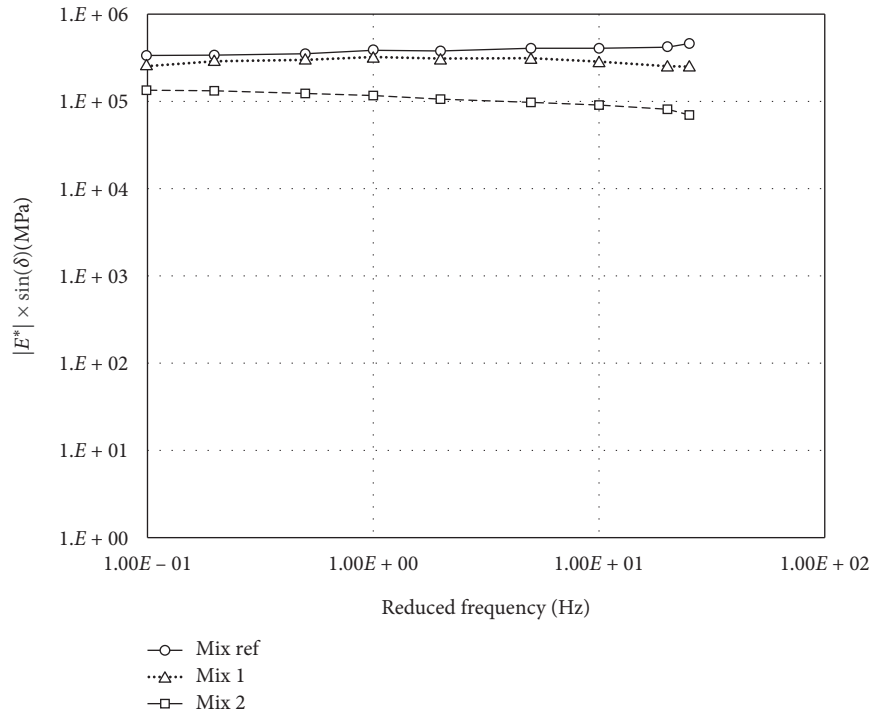


FIGURE 8: Phase angle master curves.

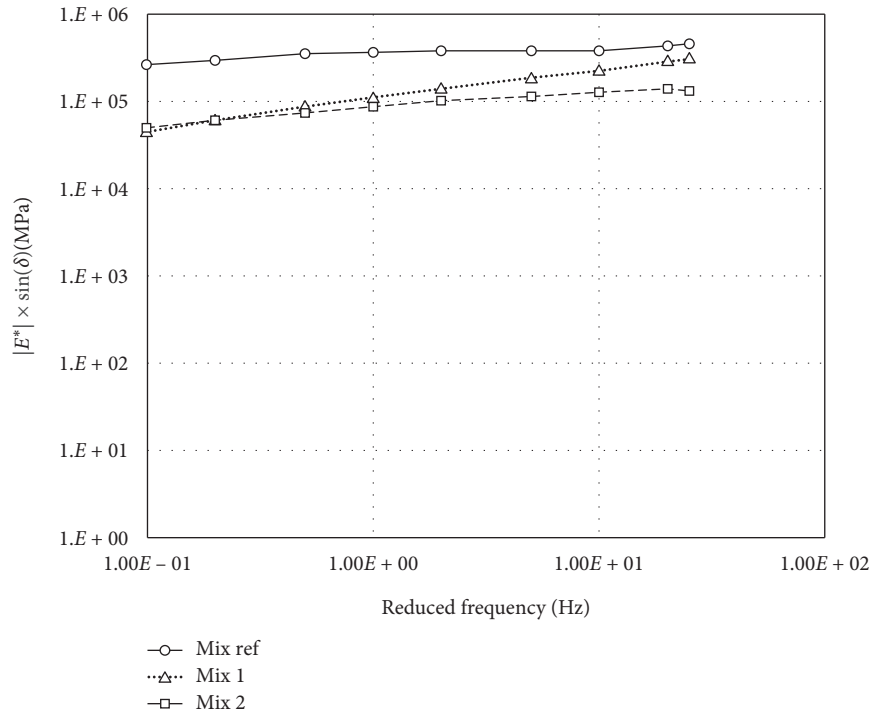
4.3. *Fatigue Resistance.* Fatigue is one of the most common damages to asphalt pavements. Generally, the occurrence and propagation of cracks are always related to the amount of energy loss caused by external loads. Fatigue parameter ($E^* \times \sin \delta$) is an effective parameter to characterize the

antifatigue performance of asphalt mixture. The values of the fatigue parameters for all mixtures (at 5°C, 20°C, and 31°C) are presented in Figure 9.

Mix ref shows the worst resistance to fatigue damage under the three temperature conditions, showing that the

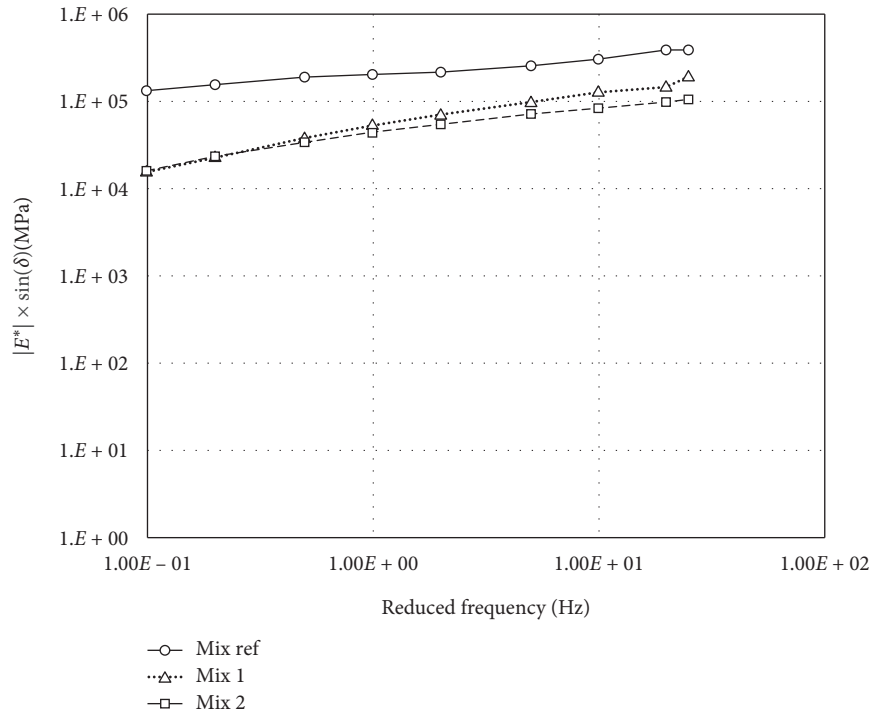


(a)



(b)

FIGURE 9: Continued.



(c)

FIGURE 9: Fatigue parameters at (a) 5°C, (b) 20°C, and (c) 31°C.

DAMs are less prone to fatigue damage than the traditional one. In fact, the higher loss factor of DAMs (Figure 8) is not conducive to the antifatigue performance, but the lower stiffness modulus (Figure 7) over the entire temperature and loading frequency ranges results in the lower fatigue parameters. In any cases, the results obtained clearly show no problems pertaining to fatigue damage for the two mixes.

At 5°C, the fatigue parameters of Mix 1 and Mix ref are similar and higher than Mix 2. This may be caused by the higher rubberized binder in Mix 2 to obtain higher damping characteristics. As the frequency increases, the fatigue parameters of Mix ref are basically at a constant level, while DAMs (Mix 1 and Mix 2) show a decreasing trend. This is because the low frequency promotes the mixture to become stiffer and more prone to fatigue cracking at low temperatures. Since the binder content in Mix ref is lower, its viscoelasticity is not obvious but closer to elasticity, so its fatigue parameters show a basically constant level.

At 20°C and 31°C, as the frequency increases, the fatigue parameters of the three mixtures all increase. As the frequency increases, the fatigue parameters of the three mixtures all increase. This is because at higher temperatures, the mixture exhibits time-dependent characteristics—the higher loading frequency increases the phase angle of the mixture, which in turn increases the fatigue parameters. In addition, the higher antifatigue performance of DAMs may also benefit from the adding of rubberized asphalt, which has been confirmed in the previous studies [35–37].

4.4. Rutting Resistance. The rutting parameter $E^*/\sin \delta$ represents the resistance to the permanent deformation of the asphalt mixture. The high complex dynamic modulus and low phase angle are conducive to the performance of the asphalt mixture at the high-temperature, reducing high-temperature flow deformation and increasing the resistance to permanent deformation. Figure 10 presents the rutting parameters of the three asphalt mixtures at 5°C, 20°C, and 31°C, respectively.

As the frequency increases, the rutting parameters of the three mixtures increase. This is because a shorter loading time means that the mixture became more stiffened and the ability to resist permanent deformation was then improved. The evolution trends of all curves are similar, but it should be noted that, under higher temperature conditions (20°C and 31°C), the difference of the rutting parameters between DAMs and traditional asphalt mixtures was more obvious.

Compared with Mix ref, DAMs (Mix 1 and Mix 2) obviously have a lower rutting parameter, indicating that its ability to resist rutting is weaker than that of traditional asphalt mixtures. This can be explained as follows: the large film thickness of mortar coating the aggregates in DAMs reduces the grain-to-grain contact in the aggregates skeleton and thus decreasing the stability of the mixture, which worsens the rutting resistance. Therefore, although the DAMs have resulted in being effective in absorbing vibrations when adopted in road pavements and track beds, the assessments of the ability to resist rutting need to be developed and the related mechanism should be analyzed as well in the future.

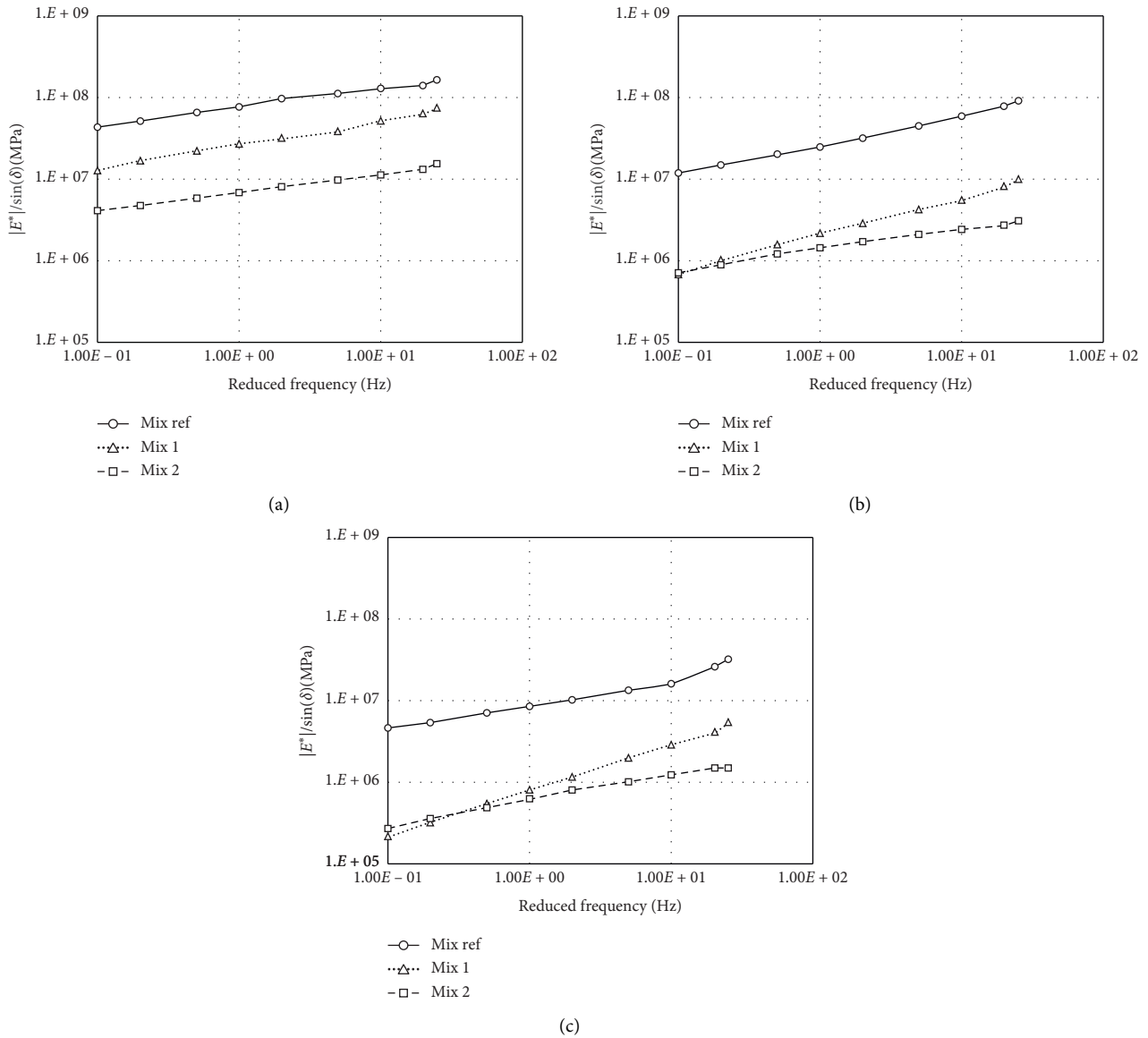


FIGURE 10: Rutting parameters at (a) 5°C, (b) 20°C, and (c) 31°C.

5. Conclusion

Viscoelastic analysis about the so-called DAMs that aim at reducing the traffic-induced vibration is presented in the present paper. The mix-design method of DAMs is based on the concept that high volumes of rubberized binder (wet method) in asphalt mixtures increase their damping response decreasing the vibratory mechanism under dynamic loading, while the excessive binder content can surely affect the viscoelastic properties of designed mixture. Focusing on viscoelastic properties, the following conclusions can be made based on dynamic mechanical testing:

The mix-design properties of the DAMs mixture meet the specification requirements, without the risk of cracking and water damage. The proposed mix-design method dedicated to DAMs is feasible. The reduction in the tensile

strength in DAMs is caused by the high volume of asphalt reducing the aggregate interlock. While the higher amount of binder and filler in DAMs tend to increase the thickness of the mastic film coating the aggregates, it improves the moisture susceptibility.

Mix ref shows the highest level of stiffness in the considered frequency range, which is in agreement with the tensile strength values and depends on the higher aggregate interlock, provided a thinner film of mastic. The stiffness difference between DAMs and Mix ref is marked in the low-frequencies region where the aggregate structure is more significant than the mastic. Mix 1 and Mix 2 show similar levels of stiffness in the intermediate and low range of frequencies with Mix 1 becoming stiffer at lower temperatures (higher frequencies) and Mix 2 stiffer at higher temperatures (lower frequencies).

Phase angle master curves of DAMs show typical shape of conventional mixtures. At low-frequency region, DAMs and conventional mix show analogous trend due to the similar skeleton structure. At the intermediate-frequency region, the phase angle is controlled by both the aggregate skeleton and the mastic showing a visible time dependency; hence, the higher amount of binder makes the mixture more temperature-susceptible and moves the peak towards higher frequencies (or lower temperatures). DAMs show consistently higher phase angle values than the reference mixture, indicating a more viscous response under loading with a consequent higher dissipation of energy.

DAMs show good resistance to fatigue damage, which may be due to the lower stiffness modulus. In the low-temperature range, with the increasing of the frequency, the fatigue parameters of Mix ref are basically at a constant level, while DAMs show a decreasing trend; while at the high-temperature range, as the frequency increases, the fatigue parameters of the three mixtures all increase.

From the results of the rutting parameters, the ability to resist rutting for DAMs is weaker than that of traditional asphalt mixtures, caused by the large film thickness of mortar coating the aggregates in DAMs reducing the grain-to-grain contact in the aggregate skeleton and thus decreasing the stability of the mixture. In the future, more assessments on the ability to resist rutting need to be developed and the related mechanism should be analyzed as well. Some initiatives to improve the rutting resistance should also be raised.

Data Availability

No data were used to support this study.

Conflicts of Interest

The authors declare no conflicts of interest.

Acknowledgments

This research was funded by the the Faculty Start-up Grant of China University of Mining and Technology (Grant No. 102520282). The authors are grateful to the colleagues from the University of Pisa for the experiment.

References

- [1] M. Browne, J. Allen, T. Nemoto, D. Au, and J. Visser, "Reducing social and environmental impacts of urban freight transport: a review of some major cities," *Procedia—Social and Behavioral Sciences*, vol. 39, pp. 19–33, 2012.
- [2] P. Clemente and D. Rinaldis, "Protection of a monumental building against traffic-induced vibrations," *Soil Dynamics and Earthquake Engineering*, vol. 17, no. 5, pp. 289–296, 1998.
- [3] O. Hunaidi and M. Tremblay, "Traffic-induced building vibrations in Montréal," *Canadian Journal of Civil Engineering*, vol. 24, no. 5, pp. 736–753, 1997.
- [4] D. Ouis, "Annoyance from road traffic noise: a review," *Journal of Environmental Psychology*, vol. 21, no. 1, pp. 101–120, 2001.
- [5] O. Hunaidi, *Traffic Vibrations in Buildings*, Citeseer, Princeton, NJ, USA, 2000.
- [6] S.-H. Ju and S.-H. Ni, "Determining Rayleigh damping parameters of soils for finite element analysis," *International Journal for Numerical and Analytical Methods in Geomechanics*, vol. 31, no. 10, pp. 1239–1255, 2007.
- [7] H. Hao, T. C. Ang, and J. Shen, "Building vibration to traffic-induced ground motion," *Building and Environment*, vol. 36, no. 3, pp. 321–336, 2001.
- [8] U. Sandberg, "Low noise road surfaces. A state-of-the-art review," *Journal of the Acoustical Society of Japan*, vol. 20, no. 1, pp. 1–17, 1999.
- [9] M. O. Al-Hunaidi, J. H. Rainer, and M. Tremblay, "Control of traffic-induced vibration in buildings using vehicle suspension systems," *Soil Dynamics and Earthquake Engineering*, vol. 15, no. 4, pp. 245–254, 1996.
- [10] T. Hanazato, K. Ugai, M. Mori, and R. Au, "Three-dimensional analysis of traffic-induced ground vibrations," *Journal of Geotechnical Engineering*, vol. 117, no. 8, pp. 1133–1151, 1991.
- [11] S. County, *Report on the Status of Rubberized Asphalt Traffic Noise Reduction in Sacramento County*, Sacramento County and Bollard and Brennan Inc, Sacramento, CA, USA, 1999.
- [12] Y.-H. Cho, C. Liu, T. Dossey, and B. F. McCullough, *Asphalt Overlay Design Methods for Rigid Pavements Considering Rutting, Reflection Cracking, and Fatigue Cracking*, University of Texas at Austin, Center for Transportation Research, Austin, TX, USA, 1998.
- [13] S. Schubert, D. Gsell, R. Steiger, and G. Au, "Influence of asphalt pavement on damping ratio and resonance frequencies of timber bridges," *Engineering Structures*, vol. 32, no. 10, pp. 3122–3129, 2010.
- [14] W. Wang and K. Höeg, "Cyclic behavior of asphalt concrete used as impervious core in embankment dams," *Journal of Geotechnical and Geoenvironmental Engineering*, vol. 137, no. 5, pp. 536–544, 2011.
- [15] H. Zhu and D. D. Carlson, "A spray based crumb rubber technology in highway noise reduction application," *Journal of Solid Waste Technology and Management*, vol. 27, pp. 27–32, 2001.
- [16] S. E. Paje, M. Bueno, F. Terán, R. Au, F. Pérez-Jiménez, and A. H. Martínez, "Acoustic field evaluation of asphalt mixtures with crumb rubber," *Applied Acoustics*, vol. 71, no. 6, pp. 578–582, 2010.
- [17] K. P. Biligiri, "Effect of pavement materials' damping properties on tyre/road noise characteristics," *Construction and Building Materials*, vol. 49, pp. 223–232, 2013.
- [18] X. G. Zhong, X. Zeng, and J. G. Rose, "Shear modulus and damping ratio of rubber-modified asphalt mixes and unsaturated subgrade soils," *Journal of Materials in Civil Engineering*, vol. 14, no. 6, pp. 496–502, 2002.
- [19] M. Rahman, G. Airey, and A. Collop, "The potentially of dry process CRM asphalt mixture as binder course and lower base layers," in *Proceedings of the Sixth International Conference on Maintenance and Rehabilitation of Pavements and Technological Control (MAIREPAV6)*, Torino, Italy, July 2009.
- [20] C. Maggiore, G. Di Mino, M. Di Liberto et al., "Mechanical characterization of dry asphalt rubber concrete for base layers by means of the four bending points tests," in *Proceedings of the 3rd Four Point Bending Beam Conference*, pp. 123–138, Davis, CA, USA, September 2012.
- [21] G. Di Mino, M. Di Liberto, C. Maggiore, and S. Au, "A dynamic model of ballasted rail track with bituminous sub-

- ballast layer,” *Procedia—Social and Behavioral Sciences*, vol. 53, pp. 366–378, 2012.
- [22] Y. Sun, G. Li, J. Zhang, and D. Qian, “Prediction of the strength of rubberized concrete by an evolved random forest model,” *Advances in Civil Engineering*, vol. 2019, Article ID 5198583, 7 pages, 2012.
- [23] Y. L. Li, Y. J. Ou, Y. Q. Tan et al., “Dynamic characteristics of rubber powder modified cement asphalt mortar,” *Advanced Engineering Forum*, vol. 5, pp. 243–246, 2012.
- [24] X. Zeng, J. G. Rose, and J. S. Rice, “Stiffness and damping ratio of rubber-modified asphalt mixes: potential vibration attenuation for high-speed railway trackbeds,” *Journal of Vibration and Control*, vol. 7, no. 4, pp. 527–538, 2001.
- [25] J. Huang, M. Losa, and P. Leandri, “Determining the effect of damping layers in flexible pavements on traffic induced vibrations,” in *Proceedings of the Advances in Materials and Pavement Prediction: Papers from the International Conference on Advances in Materials and Pavement Performance Prediction (AM3P 2018)*, pp. 255–259, CRC Press, Doha, Qatar, April 2018.
- [26] J. Huang, *Rubber Modified Asphalt Pavement Layer for Noise and Vibration Absorption*, University of Florence, Florence, Italy, 2019.
- [27] Y. Sun, J. Zhang, G. Li, Y. Wang, and C. Jiang, “Optimized neural network using beetle antennae search for predicting the unconfined compressive strength of jet grouting coalcretes,” *International Journal for Numerical and Analytical Methods in Geomechanics*, vol. 43, no. 4, pp. 801–803, 2019.
- [28] B. S. Underwood and Y. R. Kim, “Experimental investigation into the multiscale behaviour of asphalt concrete,” *International Journal of Pavement Engineering*, vol. 12, no. 4, pp. 357–370, 2011.
- [29] P. S. Kandhal and S. Chakraborty, “Effect of asphalt film thickness on short- and long-term aging of asphalt paving mixtures,” *Transportation Research Record: Journal of the Transportation Research Board*, vol. 1535, no. 1, pp. 83–90, 1996.
- [30] D. W. Christensen and R. Bonaquist, “VMA: one key to mixture performance,” *National Superpave News*, vol. 4, pp. 6–7, 2005.
- [31] J. D. Ferry, *Viscoelastic Properties of Polymers*, John Wiley and Sons, Hoboken, NJ, USA, 1980.
- [32] M. Zeng, H. U. Bahia, H. Zhai et al., “Rheological modeling of modified asphalt binders and mixtures (with discussion),” *Journal of the Association of Asphalt Paving Technologists*, vol. 70, 2001.
- [33] J. Huang and Y. Sun, “Effect of modifiers on the rutting, moisture-induced damage, and workability properties of hot mix asphalt mixtures,” *Applied Sciences*, vol. 10, no. 20, p. 7145.
- [34] C. Sangiorgi, P. Tataranni, A. Simone, V. Au, C. Lantieri, and G. Dondi, “Stone mastic asphalt (SMA) with crumb rubber according to a new dry-hybrid technology: a laboratory and trial field evaluation,” *Construction and Building Materials*, vol. 182, pp. 200–209, 2018.
- [35] L. G. R. De Mello, M. M. de Farias, and K. E. Kaloush, “Effect of temperature on fatigue tests parameters for conventional and asphalt rubber mixes,” *Road Materials and Pavement Design*, vol. 19, no. 2, pp. 417–430, 2018.
- [36] G. G. Al-Khateeb and K. Z. Ramadan, “Investigation of the effect of rubber on rheological properties of asphalt binders using superpave DSR,” *KSCE Journal of Civil Engineering*, vol. 19, no. 1, pp. 127–135, 2015.
- [37] K. E. Kaloush, “Asphalt rubber: performance tests and pavement design issue,” *Construction and Building Materials*, vol. 67, pp. 258–264, 2014.